HiJASE
Himalayan Journal of Applied Science and Engineering (A peer-reviewed Journal)

ISSN 2738-9898 (Print) ISSN 2738-9901 (Online)

Analytical and Numerical Approach for Estimating Geometry and Performance of Thrust Generating Combustion Chamber

Aplesh Kumar Mahato, Dinanath Sharma, Niraj Bhaatt, Rajeshwor Koirala, Durga Bastakoti*

Department of Mechanical and Automobile Engineering, IOE - Pashchimanchal Campus, Tribhuvan University, Pokhara, Nepal

*E-mail: *durgabastakoti@gmail.com*

Received on: 25th Oct., 2021

Accepted for publication: 30stNov., 2021

Abstract

The thrust generation capacity of any propulsion system is heavily dependent upon the geometry, flow, and performance parameters of the system. The performance parameters include temperature, pressure, and velocity estimations at the critical the locations of the systems. For the estimation of geometry and performance of thrust generating combustion chamber analytical and numerical approaches are used. Cases of under-expansion and perfectly expansion for nozzle is analysed with the theoretical calculation from which length and diameter of chamber, throat diameter, nozzle exit area are calculated and obtained as 70 mm, 70.67 mm, 21 mm and 150 mm^2, respectively for the case of under-expansion. Likewise, pressures and temperatures in the chamber, throat, and exit of the nozzle are obtained as 71.4556 bar, 40.3 bar, 59.546 bar, and 2243 K, 2238 K, 1103.511 K respectively. This also yielded that the exhaust velocity is supersonic with the value of 476.1 m/s. Values obtained for the case of perfectly expanded nozzle suggests that the geometrical dimensions of nozzles are highly reduces, performance parameters are almost the same and the exhaust velocity is increased by more than 300 %. Numerical modeling in ANSYS Fluent was performed based on the values suggested by theoretical approach. Results of numerical modeling were in close resemblance with that of the theoretical approach suggesting validation of the simulation. Pressure, temperatures and velocities at different locations within the combustion chamber are also obtained from numerical modeling.

Keywords: Combustion chamber, nozzle, numerical analysis, propellant, thrust.

1. Introduction:

Thrust that is generated by the propulsion system of the aircraft moves it through the air. Different propulsion systems develop thrust in different ways, but all thrust is generated through some application of Newton's third law of motion, for every action there is an equal and opposite reaction. In any propulsion system, a working fluid is accelerated by the system and the reaction to this acceleration produces a force on the system. NASA defines the propulsion as a machine that produces thrust to push an object forward [1]. An aircraft propulsion system must achieve two things. First, the thrust from the propulsion system must balance the drag of the airplane when the airplane is cruising. And second, the thrust from the propulsion system must exceed the drag of the airplane for the

airplane to accelerate. The greater the difference between the thrust and the drag, called the excess thrust, the faster the airplane will accelerate. The phenomena of combustion are of prime importance in any thruster or propulsion system. A jet exhaust produces a net thrust from the energy obtained from combusting fuel which is added to the inducted air. This hot air passes through a high-speed nozzle, a propelling nozzle, which enormously increases its kinetic energy [2].

In this research, de- Laval nozzle is used which is Convergent-Divergent (CD) type. CD nozzles can accelerate fluids that have choked in the convergent section to supersonic speeds and this process is more efficient than allowing a convergent nozzle to expand supersonically externally. The shape of the divergent section also ensures that the direction of the escaping gases is directly backwards, as any sideways component would not contribute to thrust [3]. Shi X. et al. performed study on modes of reaction front propagation and end-gas combustion of hydrogen/air mixtures in a closed chamber [4]. Likewise, Gao W. et al. studied the effects of particle characteristics on flame propagation behavior during organic dust explosions in a half-closed chamber [5]. Noor M. M. et al. [6] conducted a preliminary study of control parameters for open furnace mild combustion using Computational Flow Dynamics (CFD). Ozsezen A. N. et al. [7] studied the performance and combustion characteristics of alcohol–gasoline blends at wide-open throttle. Likewise, another work done in liquid rocket engine has also focused on complicating factors of chemical kinetics, highly nonlinear source terms, and sub-grid scale velocity and scalar-missing interactions and performed modeling high-pressure mixing and combustion processes in liquid rocket engines [8]. Liang K. et al. [9] performed an investigation of Heat Transfer and Coking Characteristics of Hydrocarbon Fuels. Similarly, Son M. et al. [10] performed a numerical study on the combustion characteristics of a fuel-centered injector for methane rocket engines. In this study, combustion simulation was conducted using methane and oxygen to determine the effects of injection condition and geometries upon combustion characteristics. They suggested that there is recent research works are going in the direction on advancement of performance and simplification on designing of propulsion system. In another work, Lux J. et al. concluded that flame stabilization is one of the prime parameters of nozzle functioning which is directly dependent on the flame temperature. Another research performed temperature estimation in the combustion chamber of internal combustion engine which used the mathematical model of heat transfer phenomena [12]. This helped the project on further analysis of heat transfer and combustion chamber geometry estimation which tend to establish the optimization technique in solving the problem numerically.

All these suggested that research in combustion chamber with nozzle is still not saturated and theoretical and numerical modeling is needed to address the issues for estimating design and performance parameter. This research work focuses on obtaining optimum design of geometry of the thruster and obtains the performance of a thrust generating combustion chamber. For this aim, theoretical approach is chosen to obtain the diameter of combustion chamber, throat and nozzle theoretically. It is also intended to obtain the pressure, temperature and velocity of gases inside the chamber at critical locations theoretically followed by numerical analysis of geometry under the initial conditions of temperature and pressure which is 303 K and 140 psi along with propellant combinations of liquefied petroleum gas (LPG) butane and oxygen as fuel. Solid works 2020 was used for 2D and 3D modeling of the system, and ANSYS 2020 was used for finite element analysis of the analytical model.

2. Analytical and Numerical Approach:

Analytical approach is the exact approach that comprises use of theoretical equations of different discipline used to model the system. Numerical approach basically represents approximation methods for solving a given problem. Governing equations are used to solve the problem in that particular domain which include conservation of mass, momentum, energy, species and effect of body forces.

2.1. Analytical Approach:

The function of a chemical thruster is to generate thrust through chemical combustion reaction with release of the thermal energy derived from the chemical reaction undergoing between propellants that yields high-temperature and high-pressure gases. Thermo-chemical properties for the calculation of design and performance parameters including the formation of these exhaust gases are considered for two cases of under expansion and perfectly expansion.

Predefined Performance of Propellants Combinations

Fuel & Oxidizer : LPG (Butane) & Industrial Oxygen

Feed Pressure [P_f]: 70 psi (Butane) + 70 psi (Oxygen) = 9.652664 bar

Feed Temperature [T_f]: 303 K

Stoichiometry of Propellant Combustion Process

For a complete combustion process, Butane burns in the presence of oxygen and gives out carbon-dioxide and water vapour as by-product. The chemical equation can be given as (Eq. 1)

$$aC_4H_{10} + bO_2 \rightarrow cCO_2 + eH_20 \quad (1)$$

Balancing Eq. 2 for 1 mole of butane,

$$C_4H_{10} + 6.5O_2 \rightarrow 4CO_2 + 5H_20 \quad (2)$$

Mixture ratio for Eq. 2 chemical reaction can be given by Eq. 3 as:

$$r = \frac{weight\ \ of\ \ oxidizer}{weight\ \ of\ \ fuel} = \frac{n_{O_2} M_{O_2} * g}{n_{C_4H_{10}} M_{C_4H_{10}} * g} \quad (3)$$

The temperature inside the combustion chamber is assumed to be 2243 K so,

T_c = 2243 K [16]

The pressure inside the combustion chamber after the combustion process varies according as the temperature varies after combustion and is dependent of feed pressure and feed temperature. So, the pressure inside a combustion chamber can be given by Eq. 4.

$$P_c = P_f \left[\frac{T_c}{T_f} \right] \quad (4)$$

The Pressure at the exit of the nozzle (P_e) can be co-related with the chamber pressure as

$$P_e = k * P_c \quad (5)$$

where, k = (no. of moles of reactant) / (no. of moles of product) = 0.8333

Similarly, temperature at the exit of nozzle after expanding in the divergent section following a polytropic process can be given by Eq. 6 as

$$T_e = T_c \left[\frac{P_e}{P_c} \right]^{\frac{\gamma-1}{\gamma}} \quad (6)$$

The pressure and temperature of gases can be given by the Eq. 7 and Eq. 8, respectively As:

$$P_t = P_c \left[1 + \frac{\gamma - 1}{2} \right]^{-\frac{\gamma}{\gamma-1}} \quad (7)$$

$$T_t = T_c \left[\frac{1}{1 + \frac{\gamma - 1}{2}} \right] \quad (8)$$

Effective Average Molecular Mass [$\Im$] is the average effective mass of the molecules of the gas taking part in the chemical reaction which can be given by Eq. 9

$$\Im = \frac{\sum_{i=1}^{m} n_i M_i}{\sum_{j=1}^{m} n_j} \quad (9)$$

where, M_i is molecular mass of reactants; n_i and n_j are number of moles of reactants and products The pressure of the exhaust gases at the exit of the nozzle is a critical factor that determines the nature of the flight i.e., either a perfectly expanded nozzle ($P_e = P_{atm}$) or, under-expanded nozzle ($P_e > P_{atm}$) or, over-expanded nozzle ($P_e < P_{atm}$). Determination of the geometry of the combustion chamber and nozzle is done based on two approach viz. under-expanded nozzle

approach and perfectly expanded nozzle approach.

2.2. Under-Expanded Nozzle Approach:

In this approach, P_e = 59.546 bar [From Eq. 5] is taken and further is study is done to calculate the geometry of the nozzle. Different performance parameters are also discussed.

2.2.1. Exhaust Velocity [*U*]:

It is the average velocity of the burnt gases leaving out the nozzle. It is responsible for the generation of the thrust and specific impulse and can be given by Eq. 10

$$U = \sqrt{\frac{2\gamma}{\gamma-1}\frac{R'T_c}{\Im}\left[1-\left(\frac{P_e}{P_c}\right)^{\frac{\gamma-1}{\gamma}}\right]} \quad (10)$$

Where, γ = 1.2 Specific Heat Ratio; R = 8314.3 J g^{-1} K^{-1} Gas Constant

2.2.2. Specific Impulse [I_{sp}]:

It is a measure of how efficiently a reaction mass engine creates thrust which is exactly proportional to exhaust gas velocity. Specific Impulse for this system is given by Eq.11

$$I_{sp} = \frac{U}{g} \quad (11)$$

2.2.3. Thrust Calculation:

It is the force required to overcome its body weight. For M = 16 kg, being the sum of mass of the entire component in the workbench with the overload factor (factor of safety = 1.25), M = 1.25 × 16 = 20 kg. Hence,

$$F = \psi * M * g \quad (12)$$

where, ψ is the thrust to weight ratio.

2.2.4. Total Propellant Weight Flow Rate [w_t]:

The amount of reaction product leave-out from the engine in given time and it is given by ratio of force with specific impulse.

$$w_t = \frac{F}{I_{sp}} \quad (13)$$

2.2.5. Total Propellant Mass Flow Rate [m_t]:

The sum of mass flow rate of the propellant i.e., fuel (Eq. 15) and oxygen (Eq. 16) is named as total propellant mass flow rate which is given by Eq. 14

$$m_t = \frac{w_t}{g} \quad (14)$$

2.2.6. Mass of Fuel Flow Rate [m_f]:

$$m_f = m_t\left[\frac{1}{r+1}\right] \quad (15)$$

2.2.7. Mass of Oxygen Flow Rate [m_o]:

$$m_o = m_t\left[\frac{r}{r+1}\right] \quad (16)$$

2.2.8. Effective Exhaust Velocity [*c*]:

It is effective velocity of the exit hot gas that produces the thrust. For optimum operation, it is considered that the exit P_e=P_a=101325P (given by Eq. 11).

The schematic diagram of the nozzle is given in Fig. 1 which represents the geometrical parameters requirement to obtain the geometry of the nozzle.

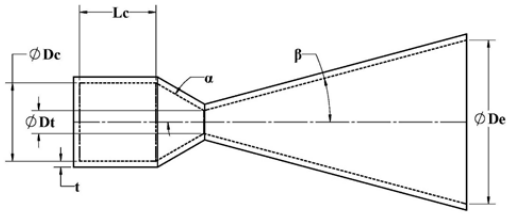

Figure 1: Labeled geometry of the chamber-nozzle

2.2.9. Nozzle Throat Cross Section Area [A_t] & Diameter [D_t]:

The throat area can be given as a function of mass flowrate of propellant, chamber pressure, effective average molecular mass and chamber temperature as given in Eq. 17 and the diameter of throat by Eq. 18

$$A_t = \frac{m_t}{P_c\left\{\gamma\left(\frac{2}{\gamma+1}\right)^{\frac{\gamma+1}{\gamma-1}}\frac{\Im}{R'T_c}\right\}^{\frac{1}{2}}} \quad (17)$$

$$D_t = \sqrt{\frac{4*A_t}{\pi}} \quad (18)$$

2.2.10. Mach Number at the Nozzle Exit [M_e]

Mach number shows the velocity of that gas against the velocity of the sound. In this case, Mach number is given by the function of chamber pressure and atmospheric pressure as stated in Eq.19

$$M_e = \left[\frac{2}{\gamma - 1} \left\{ \left(\frac{P_c}{P_{atm}} \right)^{\frac{\gamma-1}{\gamma}} - 1 \right\} \right]^{\frac{1}{2}} \quad (19)$$

2.2.11. The Nozzle Exit Area [A_e] and Diameter [D_e]:

The nozzle exit area and diameter can be given by Eq. 20 and Eq. 21 as:

$$A_e = \left[\frac{A_t}{M_e} \left\{ \frac{1 + \left(\frac{\gamma - 1}{2} \right) M_e^{\,2}}{\left(\frac{\gamma + 1}{2} \right)} \right\}^{\frac{\gamma+1}{2(\gamma-1)}} \right]^{\frac{1}{2}} \quad (20)$$

$$D_e = \sqrt{\frac{4 * A_e}{\pi}} \quad (21)$$

2.2.12. Temperature at the Nozzle Exit [T_e]:

The temperature of exhaust gases at the exit of nozzle can be correlated with chamber pressure, chamber temperature and exit pressure via polytrophic expansion process which is given in Eq. 22.

$$T_e = T_c \left(\frac{P_e}{P_c} \right)^{\frac{\gamma-1}{\gamma}} \quad (22)$$

2.2.13. Characteristics Chamber Length [L^*]

Characteristics chamber length is the imaginary length of combustion chamber suitable enough for a complete combustion process. Based on the characteristics of the engine, it can be chosen as L^* = 1.016 m

2.2.14. Combustion Chamber Volume [V_c]

The volume of combustion chamber can be given by the Eq. 23

$$V_c = L \times A_t = 0.000358885 \text{ m}^3 \quad (23)$$

2.2.15. Combustion Chamber Length and Diameter [L_c]

The length and diameter of the combustion chamber are correlated with volume of combustion chamber. Since the Volume of combustion chamber also includes the conical convergent section, depending on the angle of convergence, β . The volume of the combustion chamber can be given by Eq. 24.

$$V_c = \frac{\pi D_c^{\,2}}{4} L_c + \frac{1}{3} * \frac{(D_c/2)^2 - (D_t/2)^2}{\tan\beta} \quad (24)$$

Rearranging the equation to solve for chamber diameter

$$D_c = \sqrt{\frac{D_t^{\,3} + \frac{24}{\pi} \tan\beta * V_c}{D_c + 6 \tan\beta * L_c}} \quad (25)$$

approximating a second order value for L_c=0.070 m and β =30° iterating the above equation, D_c=0.07167 m (sixth iteration) which satisfy the Eq. 25.

2.2.16. Length of Convergent Section [L_{cs}]

It is the axial length of the convergent section of the nozzle and is calculated as:

$$L_{cs} = \frac{D_c/2 - D_t/2}{\tan\beta} \quad (26)$$

2.2.17. Length of Divergent Section [L_{ds}]

It is the axial length of the divergent section of the nozzle and can be given as:

$$L_{ds} = \frac{D_e/2 - D_t/2}{\tan\alpha} \quad (27)$$

where α =15° is the angle of divergence

2.2.18. Molecular Stay Time in the Combustion Chamber [t_s]

It is time taken by the molecules of the gases inside the combustion chamber for a complete combustion process and can be given by the Eq. 30.

$$r' = \frac{P_c \Im}{R' T_c} \tag{28}$$

$$V = \frac{1}{r'} \tag{29}$$

where r' is the specific volume of the gases taking part in chemical reaction; and V is the density of the gases

$$t_s = \frac{V_c}{\dot{m} V} \tag{30}$$

2.2.19. Thickness of the Combustion Chamber [t_w]:

The engine is made from stainless steel (Astm304) σ_{ult}=82.4 psi. Allowable stress is given by Eq. 2.31 as:

$$\sigma_{all} = \frac{\sigma_{ult}}{f} \tag{31}$$

where, is the factor of safety with value 6, and thickness of the combustion chamber can be obtained as:

$$t_w = P_c \frac{D}{\sigma_{all}} f \tag{32}$$

2.3. Perfectly Expanded Nozzle Approach:

In this approach, $P_e = P_{atm}$ = 1 bar is taken and further is study is done to calculate the geometry of the nozzle. Different performance parameters are also discussed. The method of calculations is similar to the under expanded nozzle approach.

2.3.1. Thrust Calculation:

Let total mass of the rocket including nozzle and combustion chamber is 20 kg. Hence, thrust to be obtained is 3920 N. (Ψ =20 is taken)

2.3.2. Combustion Chamber Length [L_c], Area [A_c] and Diameter [D_c]

The length of the combustion chamber can be given by Eq.33

$$L_c = \frac{\frac{V_c}{A_t} - \frac{1}{3}\sqrt{\frac{A_t}{\pi}} \cot\beta \left(\varepsilon_c^{1/3} - 1\right)}{\varepsilon_c} \tag{33}$$

Where, β = 30 is angle of convergence; ε_c = 4 is contraction ratio which is the area ratio of chamber to throat. Hence, combustion chamber diameter can also be obtained as:

$$D_c = \sqrt{\frac{4 * A_c}{\pi}} \tag{34}$$

2.4. Numerical Approach:

For this problem, medium powered personal computers are used which include i5 8th generation processor and 2GB NVidia MX150 video graphics as computational machines. Of much available CFD software, the best suited ANSYS 2021 R1 is used to solve the problem.

The domain of this problem includes an inlet section, an outlet section, a nozzle wall section and a far filed section. The inlet section is one from which the fluid is feed into the domain, the outlet section is one from which the burnt gases are exhausted out from the domain, nozzle wall section is one which acts as the wall for the chamber and the nozzle, the far field section is one which defines the outside/environment condition. The boundary condition can as in terms of pressure, temperature, mass flow rate, or velocity.

The boundary conditions for before combustion fluid flow model are considered as:

(i) inlet section is defined as 9.6 bar pressure at 303K,
(ii) the wall and far field are set to adiabatic conditions,
(iii) the outlet section is defined as 1 bar pressure at 303K.

The boundary conditions for after combustion fluid flow model are taken as:

(i) inlet section is defined as 71.5 bar pressure at 2243 K,
(ii) the wall and far field are set to adiabatic conditions,
(iii) the outlet section is defined as 1 bar pressure at 303 K.

First, 2D geometry is created in modeling software with the dimensions obtained in analytical study from the first case, under expansion, from Fig. 2. Further refining of meshes was done and is shown in Figs. 4 (a) and (b). The same model is meshed for medium and

fine mesh and the parameters at the critical location are noted and compared for Grid Independent Test (GIT), results of which are shown in Table 1, Fig 3 and Fig. 4.

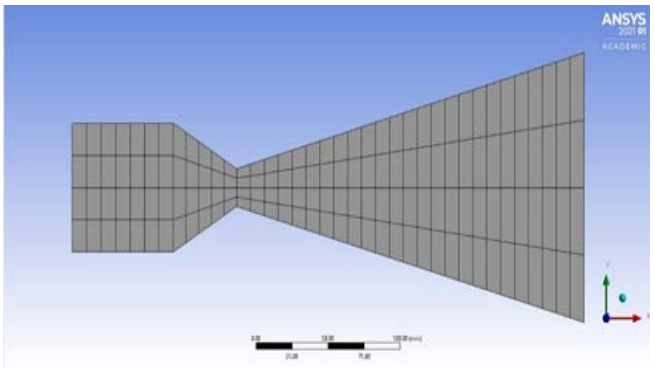

Figure 2: Mesh configuration on the basis of element size

Table 1: Velocity (m/s) parameters obtained at critical location of the geometry

Element Size (mm)	Nodes	Elements	Max velocity in domain	Min velocity in domain	Average velocity at outlet	Max velocity at outlet	Min velocity at outlet
0.01	190	148	2385.21	134.54	910.85	652.75	127.34
0.008	329	276	2038.32	22.73	761.70	877.99	28.14
0.005	675	592	2010.62	21.58	718.04	1016.89	39.26
0.004	1034	930	1943.82	19.13	677.08	1078.70	32.75
0.003	1736	1599	1922.13	16.85	639.14	1121.27	28.87
0.002	4092	3885	1894.96	10.76	581.53	1161.50	12.49

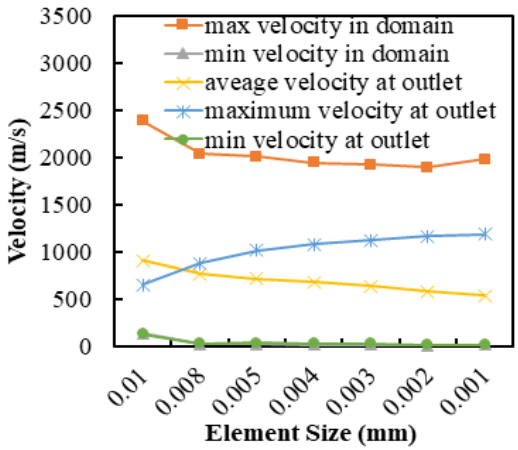

Figure 3: Parameters comparison based on different element size

Form the above GIT, element size of 0.005 mm is appropriate for the further study. Similarly, best suitable combination of the edge division is L1=L2=30, L3=120 and L4=60

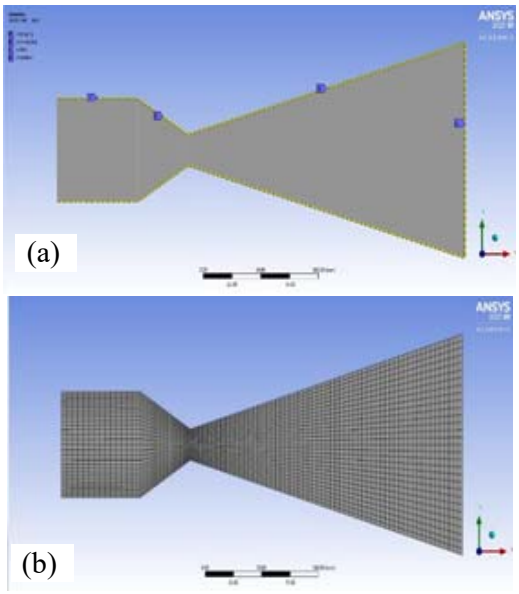

Figure 4: (a) Course mesh configuration as per number of divisions and (b) Configuration of critical edge division

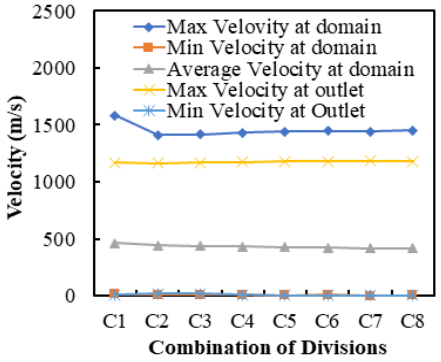

Figure 5: Results of GIT based on number of divisions

3. Results and Discussion:

3.1. Results of Analytical approach:

The geometry of the combustion chamber and nozzle along with the performance parameters contributing the nature of the flow is estimated analytically. The mixture ratio is obtained as 3.586 from Eq. 3 while combustion chamber and exit pressure is calculated to be 71.4552 bar and 59.546 bar from the Eqs. 4 and 5, respectively. The throat pressure and temperature is calculated to be 40.3 bar and 2238.88 K, respectively which are obtained using Eqs. 7 and 8. Similarly, the average molecular mass is calculated to be 29.55 gram obtained from Eq. 9. From the under expanded nozzle approach, chamber length, chamber diameter, throat diameter, nozzle exit area are calculated to be 70 mm, 70.67 mm, 21 mm, 150 mm, respectively. Pressure and temperature in the chamber, at the throat and at the exit of the nozzle are 71.4556 bar, 40.3 bar, 59.546 bar and 2243 K, 2238 K, 1103.511 K, respectively. And the exhaust velocity of 476.1 m/s is obtained. Geometrical design with dimensions for this case is represented in Fig. 6. From the perfectly expanded nozzle approach, chamber length, chamber diameter, throat diameter, nozzle exit areas are all lower than the case of under expansion and it is represented in Fig. 7. However the pressure and temperature at the boundary remains the same as stated in under expanded nozzle approach. Similarly, the exhaust velocity of 1961.35 m/s is obtained which is much greater as compared to another approach of analytical study.

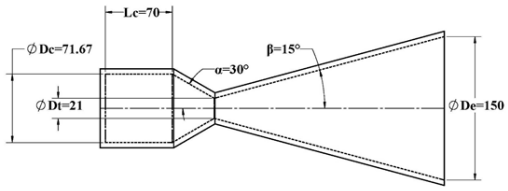

Figure 6: Detail drawing of the geometry from under-expanded nozzle approach

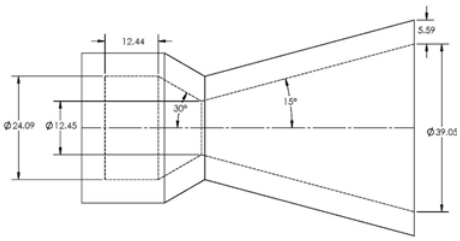

Figure 7: Detail drawing of the geometry from perfectly-expanded nozzle approach

3.2. Results of Pre-combustion:

The results from before combustion fluid flow [S1] obtained from numerical simulation are given in Fig. 8. The pressure, temperature and velocity vs axis of the geometry plot are represented in Figs. 8(a), 8(b) and 8(c). The obtained values are in coherence with the typical CD nozzle which can be seen in Fig. 9.

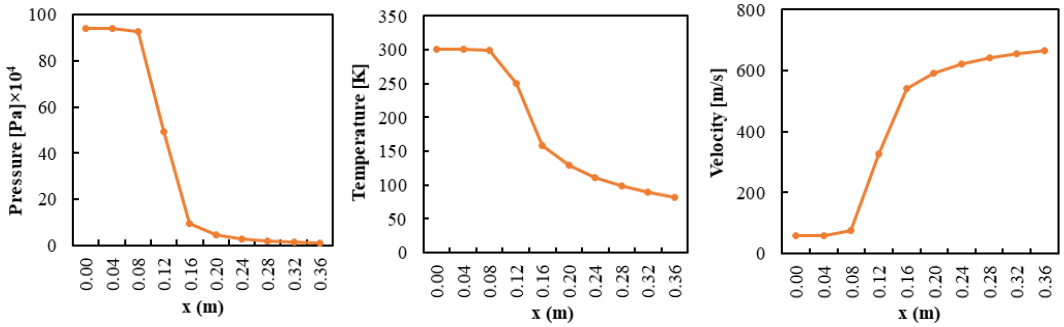

Figure 8: Plots of (a) Pressure, (b)Temperature and (c) velocity against the axis of the geometry for non-combusted fluid flow model

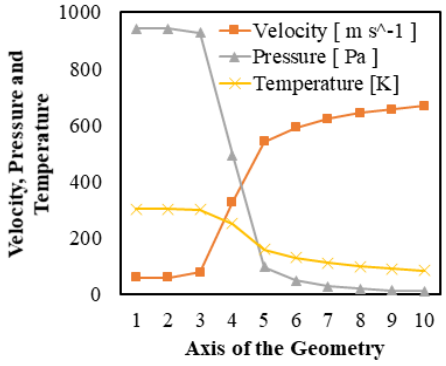

Figure 9: Combined Chart of Pressure, Velocity and Temperature along the axis the geometry

Table 2: Performance parameter at different location

	Temperature	Pressure	Velocity
Inside Chamber	300 K	9.6 bars	60 m/s
At Throat	190 K	3 bars	320 m/s
At Exit	70 K	~ 0bar	660 m/s

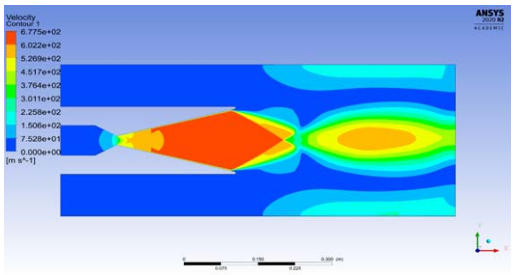

Figure 10: Velocity Contour of S1

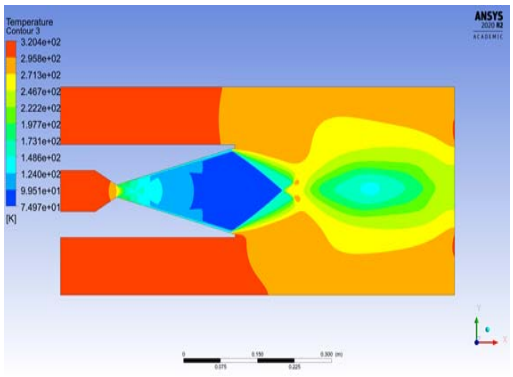

Figure 11: Temperature Contour of S1

Temperature is decreasing from chamber to exit while passing through the throat which clearly indicates the heat transfer phenomon in CD nozzle and is represented in tabular form in Table 2. Pressure is also decreasing suggesting the outward flow of exhaust. The exhaust is gaining velocity and momentum while doing so with Mach number of unity in the throat region of the nozzle which can be seen in Figs. 10, 11 and 12.

3.3. Results of Post-combustion:

The results after solving the problem to a residual of 10^{-4} by the numerical approach for the case of after combustion fluid flow model [S2] are given in Fig. 9. The velocity vector, velocity profile, temperature and pressure against the axis of the geometry are represented as contours in Figs. 13-16. In this case too, temperature and pressure are falling while passing onto the exit region of the nozzle and velocity the otherwise with Mach number more than 1 in throat.

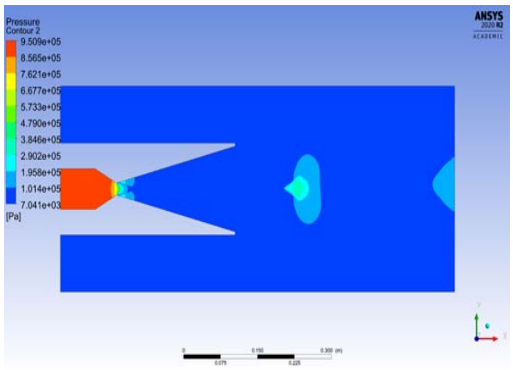

Figure 12: Pressure Contour of S1

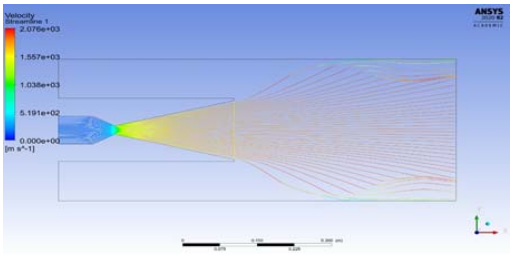

Figure 13: Velocity Vector Plot of S2

Table 3: Obtained parameter at different location of the geometry

	Temperature (K)	Pressure (Bars)	Velocity (m/s)
Inside Chamber	2250	70	180
At Throat	1800	30	800
At Exit	650	~ 1	1800

3.4. Validation of Numerical Approach:

The numerically obtained results are checked for credibility by two validation methods i.e., comparing numerical approach with published similar work-based research paper and comparing numerical approach with analytical

approach. The research paper with similar work done by Malay S. Patel's "Concepts and CFD Analysis of De-Laval Nozzle" [14] is appropriate for this validation.

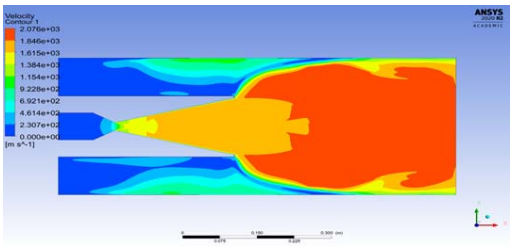

Figure 14: Velocity Contour Plot of S2

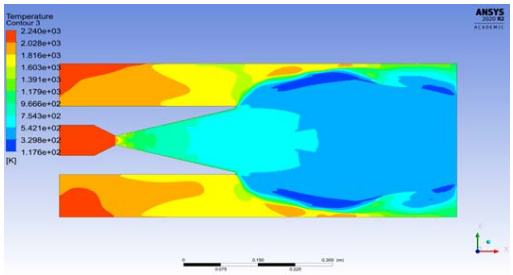

Figure 15: Temperature Contour Plot of S2

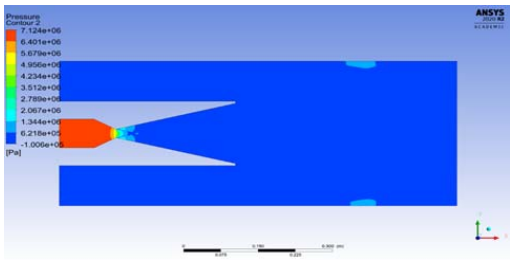

Figure 16: Pressure Contour of S2

The comparison provided the similarities in terms of parameters of this numerical approach and research paper. In the convergent part, the pressure and temperature are maintained constant so that the flame will be stable enough to be hold inside the combustion chamber as a result of that combustion process is actively running again and again which can be seen in both, in numerical approach and research paper. Reaching the throat region, there is sudden decrease in the pressure and the temperature resulting in exchange of energy, the heat energy of gases is converted into the kinetic energy of the gases as the result of that there is a sudden increase in the velocity of the gases can be seen. In the divergent section, due to the expansion process, the pressure and the temperature of the gases go on decreasing further such that normal conditions are achieved as a result of that the velocity is further increase to the maximum level.

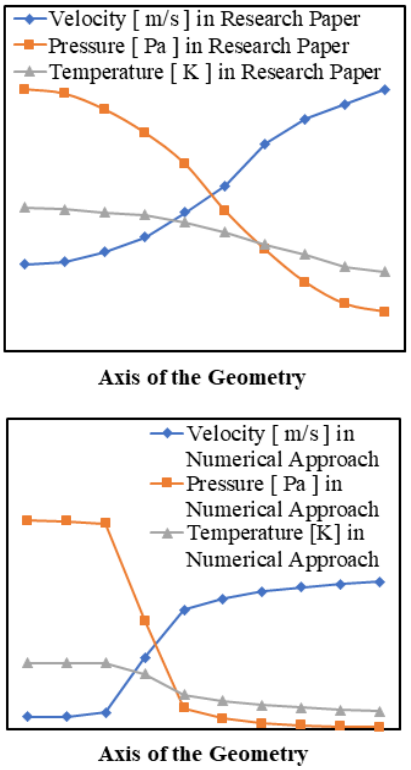

Figure 17: Pressure, velocity and temperature comparison of (a) research paper [14] and (b) results of this numerical approach

In another comparison, the results obtained from the numerical approach is compared with the results obtained from the analytical approach [16]. The nature of graph from analytical approach is similar with] the temperature and pressure goes on decreasing while velocity increases as the gas flows from the combustion chamber towards out of nozzle. And comparing Fig. 18 (a) with Fig 18 (b), similar trend can be observed.

The temperature error, pressure error and velocity error of 0.3 % (<10 %), 2 % (<10 %), 8.227 % (<10 %) are obtained in the numerical analysis. Similarly, Mach number in the convergent section is obtained as 0.625. The Mach number at the throat is obtained as 1, and the Mach number in the divergent section is obtained as 2.06 in numerical analysis. Hence numerical analysis is valid in terms of temperature, pressure, velocity and Mach number.

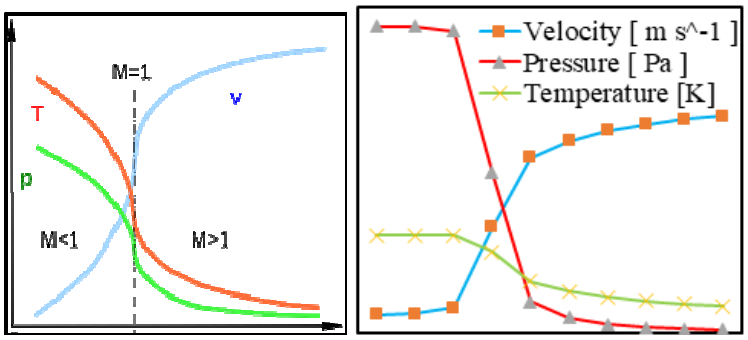

Figure 18: Velocity, Pressure and temperature plots from (a) analytical approach [16] and (b) results of this numerical approach

4. Conclusion:

Geometry of the combustion chamber and converging diverging nozzle is estimated analytically under two approaches and second approach geometry is put under finite element analysis to estimate the performance parameters numerically. Using different discipline of engineering such as gas dynamics, turbo machinery and thermodynamics the geometry and the performance parameters can be calculated. From two different approaches different geometry is calculated. From first approach also called as under expanded nozzle approach, chamber length, chamber diameter, throat diameter, nozzle exit area are calculated to be 70 mm, 70.67 mm, 21 mm, 150 mm resp. Pressure and Temperature in the chamber, at the throat and at the exit of the nozzle are 71.4556 bar, 40.3 bar, 59.546 bar and 2243 K, 2238 K, 1103.511 K, respectively. And the exhaust velocity of 476.1 m/s is obtained which is clearly more than the speed of sound in air. From the second approach, also called as perfectly expanded nozzle approach, chamber length, chamber diameter, throat diameter, nozzle exit area are calculated to be 12.44 mm, 24.09 mm, 12.45 mm, 39.05 mm, respectively, suggesting clear reduction in dimensions of CD nozzle. However, the pressure and temperature at the boundary remains the same, while the higher exhaust velocity of 1961.35 m/s is obtained. Similarly, from the numerical analysis the temperature inside the chamber, at the throat and at exit were found to be 2250 K,1800 K and 650 K, respectively. In the same way, the pressure was estimated to be 70 bar, 30 bar and 0 bar inside the chamber, at throat and at exit respectively. Likewise, the velocity inside the chamber, at throat and at exit was found to be 180 m/s, 800 m/s and 1800 m/s, respectively.

Acknowledgements:

We would like to express our sincere thanks to Department of Mechanical and Automobile Engineering, Institute of Engineering, Pashchimanchal Campus, Pokhara for providing opportunity for this research.

References:

[1] "Propulsion," NASA, 09-Jun-2015. [Online]. Available: https ://www.nasa.gov/audience/forstudents/k-4/dictionary/Propulsion.html. [Accessed: 05-Jan-2021].

[2] H. Cohen, R. G. F. C., P. Straznicky, S. H. I. H., and A. Nix, Gas turbine theory, 5th ed. Harlow, United Kingdom: Pearson, 2017.

[3] Converging diverging nozzle. [Online]. Available: https://www.engapplets.vt.edu/fluids/CDnozzle/cdinfo.html. [Accessed: 05-Jan-2021].

[4] X. Shi, J. I. Ryu, J.-Y. Chen, and R. W. Dibble, "Modes of reaction front propagation and end-gas combustion of hydrogen/air mixtures in a closed chamber," International Journal of Hydrogen Energy, vol. 42, no. 15, pp. 10501–10512, 2017.

[5] W. Gao, R. Dobashi, T. Mogi, J. Sun, and X. Shen, "Effects of particle characteristics on flame propagation behavior during organic dust explosions

in a half-closed chamber," Journal of Loss Prevention in the Process Industries, vol. 25, no. 6, pp. 993–999, 2012.

[6] M. M. Noor, A. P. Wandel, and T. F. Yusaf, "A preliminary study of control parameters for open furnace mild combustion using CFD," In 2nd Malaysian Postgraduate Conference, 2012

[7] A. N. Ozsezen and M. Canakci, "Performance and combustion characteristics of alcohol–gasoline blends at wide-open throttle," Energy, vol. 36, no. 5, pp. 2747–2752, 2011.

[8] J. C. Oefelein, and V. Yang, "Modeling high-pressure mixing and combustion processes in liquid rocket engines," Journal of Propulsion and Power, vol. 14, no. 5, pp. 843–857, 1998

[9] K. Liang, B. Yang, and Z. Zhang, "Investigation of heat transfer and coking characteristics of hydrocarbon fuels," Journal of Propulsion and Power, vol. 14, no. 5, pp. 789–796. 1998

[10] M. Son, K. Radhakrishnan, Y. Yoon, and J. Koo, "Numerical study on the combustion characteristics of a fuel-centered pintle injector for methane rocket engines," Acta Astronautica, pp. 135, 2017

[11] J. Lux, and O. Haidn, "Flame stabilization in high-pressure liquid oxygen/methane rocket engine combustion," Journal of Propulsion and Power, vol. 25, no. 1, pp. 15–23, 2009

[12] G. R. Safakish, "Temperature Estimation in the Combustion Chamber of an Internal Combustion Engine," Advances in Mechanical Engineering: SAGA Journals, vol. 4, 2015

[13] E. Carvajal-Trujillo, F. J. Jiménez-Espadafor. B. Villanueva et. al. "Methodology for the estimation of head inner surface temperature in an air-cooled engine," Applied Thermal Engineering, pp. 202–211, 2012 [Online]. Available: doi: 10.1016/j.applthermaleng.2011.10.032

[14] M. S. Patel, S.D. Mane, and M. Raman, "Concepts and CFD analysis of de-laval nozzle," International Journal of Mechanical Engineering and Technology, vol. 7, no. 5, pp. 221–240, 2016.

[15] "Adiabatic flame temperatures," Engineering ToolBox. [Online]. Available: https://www.engineeringtoolbox.com/adiabatic-flame-temperature-d_996.html. [Accessed: 05-Jan-2021].

[16] "Kerbal Space Program Forums," 22-Apr-2020. [Online]. Available: https://forum.kerbalspaceprogram.com/index.php?/topic/126932-ksp-inspired-me-to-design-a-liquid-fueled-rocket-engine/ [Accessed: 25-Dec-2019].